2014

Model-Based Energy Analysis of an Integrated Midrex-Based Iron/Steel Plant

AbdelHamid M. Ajbar
King Saud University, aajbar@ksu.edu.sa

Khalid I. Alhumaizi
King Saud University, humaizi@ksu.edu.sa

Moustafa A. Soliman
The British University in Egypt, moustafa.aly@bue.edu.eg

Emadadeen Ali
King Saud University, amkamal@ksu.edu.sa

Chem. Eng. Comm., 201:1686–1704, 2014

ISSN: 0098-6445 print/1563-5201 online
DOI: 10.1080/00986445.2013.825835

Model-Based Energy Analysis of an Integrated MIDREX-Based Iron/Steel Plant

A. AJBAR,[1] K. ALHUMAIZI,[1] M. A. SOLIMAN,[2] AND E. ALI[1]

[1]Department of Chemical Engineering, King Saud University, Riyadh, Saudi Arabia
[2]Department of Chemical Engineering, British University in Egypt, El Shorouk City, Egypt

This article presents modeling and simulations of an integrated plant for the production of steel using the direct reduced iron (DRI)/electric arc furnace (EAF) route. In a previous work (Alhumaizi et al., 2012), a comprehensive mathematical model of an iron plant based on MIDREX technology was developed, validated, and simulated. In this article, the model is extended to account for an empirical model of an EAF plant. Numerical simulations were carried out for the effect of different operating parameters of the integrated plant. Useful profiles as well as a summary table were compiled to illustrate the results of the sensitivity analysis. Key performance indicators of the plant include metallization degree and operating costs of the DRI and of the EAF as well as the total operating cost of the plant. The analysis allows the identification of operating parameters that can lead to a more profitable operation of the plant.

Keywords Cost analysis; Direct reduced iron; Electric arc furnace; MIDREX; Modeling; Simulations

Introduction

The iron and steel industry is one of the most energy-intensive industries, making energy a significant part of the cost in the production of steel. In countries with cheap coal, e.g., USA, Europe, and China, steel is generally produced through the blast furnace (BF)/basic oxygen furnace (BOF) route. In countries with cheap natural gas sources, e.g., the Middle East and Latin America, steel is generally produced through the direct reduced iron (DRI)/electrical arc furnace (EAF) route.

Methods to make the iron/steel industry more profitable by optimizing energy use is a subject that has been receiving increasing attention in the literature. The analysis of energy systems in the steel industry is, however, a complex task because there are a number of material and energy flows that interact in sometimes unpredictable ways. Accordingly, different approaches have been followed in the literature for energy analysis. Thermodynamic analysis (Fraser et al., 2006) and process

Address correspondence to E. Ali, Department of Chemical Engineering, King Saud University, P.O. Box 800, Riyadh, 11421, Saudi Arabia. E-mail: amkamal@ksu.edu.sa

integration (Larsson and Dahl, 2003; Larsson et al., 2006) are some of the tools used for the optimization of energy use in iron/steel plants.

A model-based approach is also a useful tool for energy analysis. The task of developing rigorous first-principles models for integrated plants is, however, quite difficult. The integrated plant consists of the reformer, DRI, and the EAF unit. These units are quite complex within themselves and are also connected to each other by recycle loops, making the modeling and the numerical simulations a challenging task. However, mathematical modeling is always useful when the model can incorporate the essential elements of the process and can be validated against plant data.

In earlier works, Alhumaizi et al. (2012) and Ajbar et al. (2011) developed, validated, and simulated a comprehensive mathematical model for an iron plant based on MIDREX technology (Midrex, Charlotte, N.C.; http://www.midrex.com). The methodology consisted in the development of rigorous first-principles models for the reformer and reduction furnace, in addition to models for auxiliary units such as the heat recuperator, the scrubber, and the compressor. In this regard, a one-dimensional heterogeneous model for the catalyst tubes that takes into account the intraparticle mass transfer resistance was developed for the reformer unit, while the furnace was modeled with bottom firing configuration. As for the reduction furnace, the mathematical model was based on the concept of the shrinking core model.

In this article, the previous model is extended to include an empirical model of the electric arc furnace. Numerical simulations of the integrated iron/steel plant were then carried out. Sensitivity analysis allows the study of the effect of key operating parameters on the performance of the plant, including the energy consumed in the EAF plant and the oxygen requirements. This allows analysis of the total operating costs of the plant and the identification of operating parameters that can lead to a more profitable operation.

Development of EAF Model

Mathematical models of the EAF are important for the prediction of energy requirements of the unit as well as the associated wastes and emissions. Despite the pervasive nature of the EAF, many physical phenomena as well as chemical reactions that take place during the melting process are not precisely known, which hinders the development of accurate first-principles models (Bekker et al., 1999; Hocine et al., 2009; Matson and Ramirez, 1999; Morales et al., 1997, 2001, 2002). The lack of knowledge of reaction mechanisms was overcome in some studies (MacRosty and Swartz, 2005, 2007) by modeling the process as equilibrium zones with mass transport limitations. Parameter estimation was carried out using industrial data. Thermodynamics-based models for the furnace were also considered (Çamdali et al., 2003). The empirical modeling of EAF has also received attention in the literature (Adams et al., 2001; Czapla et al., 2008; Köhle, 2002; Pfeifer et al., 2005). This approach seems more practical given the complexity of the physicochemical interactions occurring in the process and given the difficulties in acquiring data for reaction rates. Different correlations for the energy requirements of the EAF are available in the literature (Adams et al., 2001; Czapla et al., 2008; Köhle, 2002; Pfeifer et al., 2005). Pfeifer et al. (2005), for instance, developed empirical models to predict electrical energy requirements based on data from various EAF installations. Czapla et al. (2008), on the other hand, used genetic algorithms to estimate the model empirical parameters.

The approach followed in this article consists in developing an empirical model for the EAF unit. However, unlike most integrated plants in the world where scrap constitutes the major part of the feed, the plant under study uses a feed that consists of large proportions of DRI, i.e., in the order of 80%, with the rest being scrap. Slag, oxygen, and carbon injection practices are different when melting DRI as compared to melting 100% scrap (Kirschen et al., 2011). Although a number of empirical equations are available in the literature to describe the energy requirements of EAF, there is little work reported in the literature on using DRI compared to using scrap. One of the few works in this field is by Dressel (1999). The author compiled industrial-based data for the energy requirement of EAF and plotted it as function of the gangue content of DRI. These plots were done for three sets of metallization degree (88%, 92%, and 96%). Each set contains three lines for three basicities of the gangue (0, 0.5, and 1). Moreover, these plots correspond to a melt of 1600°C, a DRI of 1.2% carbon, and a basicity of EAF slag (CaO/SiO_2) of 2. We carried out a fitting of these plots. Since they are mostly linear, the fitting was made quite easy. The following correlation was obtained for the energy requirement W_R:

$$W_R = 390(kWh/t) + 900\frac{W_{FeO}}{G_A}(kWh/t) + 450(kWh/t)\frac{G_a + G_Z}{G_A} \tag{1}$$

where W_{FeO} is the weight of ferrous oxide, G_A is the furnace tap weight, G_a is the amount of gangue, and G_Z is the weight of calcium oxide added.

Figure 1 shows the profiles associated with Equation (1). These plots are in excellent agreement with the original plots reported by Dressel (1999). It should be noted that this correlation was based on a melt temperature of 1600°C. For higher temperatures, a term can be added, as explained by Pfeifer et al. (2005). Equation (1)

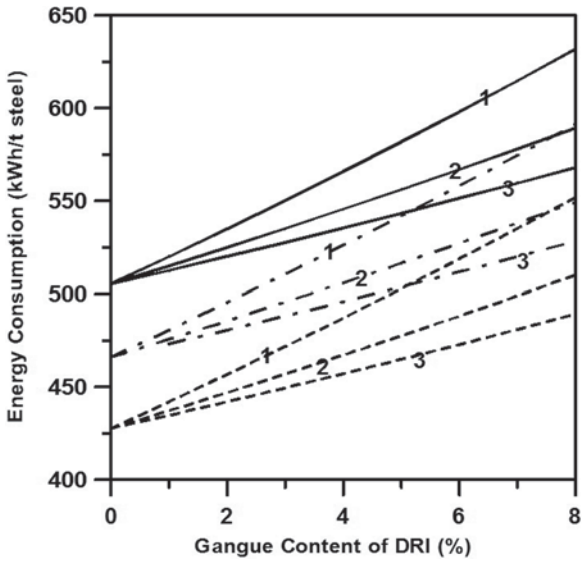

Figure 1. Plots showing the variations of energy requirements with different factors using the developed Equation (1). Curves 1: V ratio of gangue = 0; curves 2: V ratio of gangue = 0.5; curves 3: V ratio of gangue = 1; solid line, metallization degree = 88%; dash-dotted line, metallization degree = 92%; dashed line, metallization degree = 96%.

can also be further generalized to take into account the weight of carbon in DRI to yield:

$$W_R = 400(kWh/t) + 900(kWh/t)\frac{W_{FeO}}{G_A} + 450(kWh/t)\frac{G_a + G_Z}{G_A} - 800(kWh/t)\frac{W_C}{G_A} + 0.3(T - 1600)(kWh/t) \tag{2}$$

where W_C is the weight of carbon in DRI and T is the melt temperature. For the carbon content, it is known that carbon in the DRI comes from CO and CH_4. Carbon is burned in the EAF, while sometimes it is added to the unit to provide energy. In this work, complete combustion to CO_2 was assumed.

It should be noted that the developed formulas (Equations (1) and (2)) should be used along with material balance equations using the methodology proposed by Ekmekci et al. (2007). The authors modeled chemical reactions with mass conservation laws in EAF, while the chemical composition of the final steel alloy was obtained precisely according to different input compositions. The authors calculated the mass efficiency of the iron element for different input elements such as carbon, Si, and Mn. These efficiencies provide valuable information about the amount of input materials that are vanished or combusted. In this regard and in line with the work of Ekmekci et al. (2007), we have assumed that 95.9% of iron and 8.5% of carbon in the charge are recovered in the melt. The rest of the carbon is burned and supplies heat to the charge. We also assumed that 30.3% of silicon, 46.4% of manganese, 69.8% of chromium, 42.0% of sulfur, and 30.6% phosphorous of the charge go into the melt. A note should be made that CaO and MgO compounds are added to form slag with the acidic components SiO_2 and Al_2O_3 present in the DRI. In our calculations we assumed that any Al_2O_3 present is added to SiO_2 and any MgO present in the CaO feed is added to the amount of CaO.

Performance Indicators of the Integrated Plant

The objective of this study is to carry out simulations for the effect of operating parameters on the performance of an integrated plant. A number of technical performance indicators were chosen, including the degree of metallization, compression energy, energy required in EAF, and oxygen required.

Besides these technical indicators, operating costs of DRI and EAF and total operating costs of the plant were included as economic indicators. The operating cost (C_{DRI}) for the DRI production can be defined by:

$$C_{DRI} = E_C \times C_E/1000 + (f_R + f_T + f_C + f_A)C_{NG}/1000 + f_O \times C_O/1000 \tag{3}$$

where E_{C} is the compression energy, f_{R} the natural gas flow rate to the reformer, f_{T} the natural gas flow rate to the transition zone, f_{C} the natural gas flow rate to the cooling zone, f_{A} the natural gas flow rate after the reformer, f_{O} the oxygen flow rate after the reformer, C_{E} the cost of electrical energy, C_{NG} the cost of natural gas, and C_{O} the cost of oxygen. The operating cost (C_{D}) of DRI per ton of melt iron produced is therefore:

$$C_D = C_{DRI}/G_A \tag{4}$$

The operating cost (C_E) for EAF per ton of melt iron is given by

$$C_E = W_R \times C_E/1000 + O_X \times C_O/1000 \quad (5)$$

where O_X is the oxygen used in the EAF. This equation includes explicitly the cost of oxygen to burn the carbon in the DRI.

Next, we define a parameter r_f as

$$r_f = G_A/G_{A,base} \quad (6)$$

where $G_{A,base}$ is the tons of melt iron in the base case, i.e., $r_f = 1$.

The total operating cost (C_T) per ton of melt iron produced is therefore:

$$C_T = r_f \times (C_D + C_E) + (r_f - 1)(-C_P + C_L \times W_{CaO}/G_A) \quad (7)$$

where C_P is the selling price of product iron, C_L the cost of lime, and W_{CaO} is the amount in excess of G_z to form slag with the excess SiO_2. The value C_P is the credit for the excess iron produced and $C_L \times W_{CaO}/G_A$ is the cost incurred for the excess lime used to treat the excess SiO_2 in the gangue.

It can be seen from Equation (7) that as the amount of DRI produced is increased, the cost of its production and treatment in the EAF increases in proportion to the ratio (r_f) of the iron produced to the base case production. With the increase of this ratio, there is more iron and silica in the DRI than in the base case. Profit is made from the excess iron, while more CaO and MgO are to be added to form slag with the excess silica.

Simulations Studies for the Integrated Plant

Simulation studies for the plant were carried out using the parameter values shown in I–IV, which summarize the characteristics of the integrated plant. These include the design parameters of the reformer (Table I), those of the DRI furnace (Table II), the nominal operating parameters of the integrated plant (Table III), and the costs of raw materials, products, and utilities (Table IV). It should be noted that validation studies for the reformer-DRI units against a local plant were carried

Table I. Nominal values of design parameters of reformer

Parameter	Value
Reformer number of tubes	521
Reformer inside tube diameter (m)	0.2
Reformer tube thickness (m)	0.024
Reformer tube length (m)	7.9
Catalyst particle characteristic length (m)	0.0038
Catalyst pellets bulk density (kg/m^3)	250
Catalyst pore radius	80
Tortuosity	2.74

Table II. Nominal values of design parameters of DRI

Parameter	Value
Reduction furnace diameter (m)	5.5
Reduction furnace height (m)	9.1
Iron ore pellet radius (m)	0.012

Table III. Nominal values of operating parameters for the integrated reformer/DRI/EAF plant

Parameter	Value
Flow rate of hematite (Fe_2O_3) (t/h)	180.0
Flow rate of gangue (SiO_2) (t/h)	8.0
Natural gas flow rate to reformer (10^3 Nm^3/h)	22.37
Natural gas flow rate after the reformer (10^3 Nm^3/h)	2.88
Oxygen after the reformer (10^3 Nm^3/h)	1.1
Natural gas flow rate to transition zone (10^3Nm^3/h)	5.0
Natural gas flow rate to cooling zone (10^3Nm^3/h)	3.0
Fraction of scrubber exit not sent to the burner	0.73
Fraction of scrubber exit not sent to the burner and recycled to the scrubber	1/6
% Methane in natural gas	0.95

out in a previous study (Alhumaizi et al., 2012). In this article, we concentrate on the overall performance of the integrated plant.

Table V shows the results for the nominal performance of the plant. Key indicators are the degree of metallization, which is 94.7%, a reasonable value for the operation of the plant. The ratio of H_2/CO and that of $(H_2+CO)/(H_2O+CO_2)$ are respectively 1.7 and 11.5. Midrex recommends that the ratio of H_2/CO should be about 1.5. The ratio $(H_2+CO)/(H_2O+CO_2)$, on the other hand, should be between 11 and 12. Too small values reduce metallization while larger values lead to carbon deposition on the reformer catalyst. The percentage of carbon is around 2% and together with the mole fraction of CO of 31.2% suggest that at nominal operating conditions the plant is operating at reasonable conditions. The operating cost for DRI is 10.4 \$/t while the cost of the EAF is more, at 16.3 \$/t. Therefore the operating costs of EAF constitute around 60% of the total operating costs of the integrated plant.

Table IV. Unit costs

Parameter	Value
Electric energy (10^3 kWh)	\$32
Oxygen (10^3 Nm^3)	\$45
Natural gas (10^3 Nm^3)	\$26.5
Lime (t)	\$60
Product iron (t)	\$175

Table V. Performance of the integrated (reformer/DRI/EAF) plant for the nominal case

Output parameter	Value
Bustle gas temperature (K)	1200.0
Reformer inlet temperature (K)	784.0
Degree of metallization (%)	94.7
Percentage of carbon (%)	1.9
Percentage of gangue (%)	5.8
H_2/CO	1.7
$(H_2+CO)/(H_2O+CO_2)$	11.5
Compression energy (kWh)	10198.0
Energy in EAF (kWh/t melt)	496.0
Oxygen in EAF (Nm^3/t melt)	9.9
Operating costs of DRI ($/t melt)	10.4
Operating costs of EAF ($/t melt)	16.3
Total operating costs ($/t melt)	26.7
Mole fraction of H_2 in DRI	0.54
Mole fraction of CO in DRI	0.31
Mole fraction of H_2O in DRI	0.05
Mole fraction of CO_2 in DRI	0.02
Mole fraction of CH_4 in DRI	0.05

Sensitivity Analysis

Next, the effect of some input operating parameters was investigated. For each parameter a set of figures showing its effect on process output performance were generated. The variations of each parameter around the nominal value were made quite large but keeping in perspective that some bounds are to be placed on some performance outputs, e.g., the metallization degree should not go below 90%, the temperatures of the DRI should not exceed 1250 K while the ratios H_2/CO and $(H_2+CO)/(H_2O+CO_2)$ should be in the range mentioned in the previous section. Also, the mole fraction of CO_2 should not be very low to avoid carbon formation. The results of the sensitivity analysis are summarized in Table VI, where the quantitative effect of the different input parameters on the performance of the integrated plant is illustrated.

Effect of Natural Gas (NG) Flow Rate to Reformer and after Reformer

As can be seen in the summary Table VI, both of these flow rates (NG to reformer and NG after reformer) have similar effects on the plant performance. The natural gas flow rate to the reformer was varied from 21000 to 26500 Nm^3/h around the nominal value of 22370 Nm^3/h. Figure 2 shows the results of these changes. The flow rate after the reformer, on other hand, was varied from 1000 to 7100 Nm^3/h around the nominal value of 2880 Nm^3/h. The results of the sensitivity analysis of the flow rate after the reformer are shown in Figure 3.

An increase in natural gas flow rate leads initially to more reforming and more reduction. This means higher metallization, less EAF electric energy, more oxygen, more DRI operating costs, less EAF operating costs, and less total operating costs.

Table VI. Qualitative effect of the different operating parameters on the performance of the integrated plant

An increase in the variable	Metallization	Compression power	Energy in EAF	Oxygen in EAF	Operating costs in DRI	Operating costs in EAF	Total operating costs
NG to reformer	Max	+	Min	Max	+	Min	Min
NG after reformer	Max	+	Min	Max	+	Min	Min
Oxygen after reformer	+	−	−	+	+	−	−
Recycle ratio	Max	+	Min	−	+	Min	Min
Scrubber exit temp.	−	+	+	−	+	+	+
NG flow rate to cooling zone	+	+	−	+	+	−	−
NG flow rate to transition zone	+	+	−	+	+	−	−
Ratio of all flow rates	−	+	+	−	+	+	−

+: increases, −: decreases, Max: exhibits a maximum, Min: exhibits a minimum.

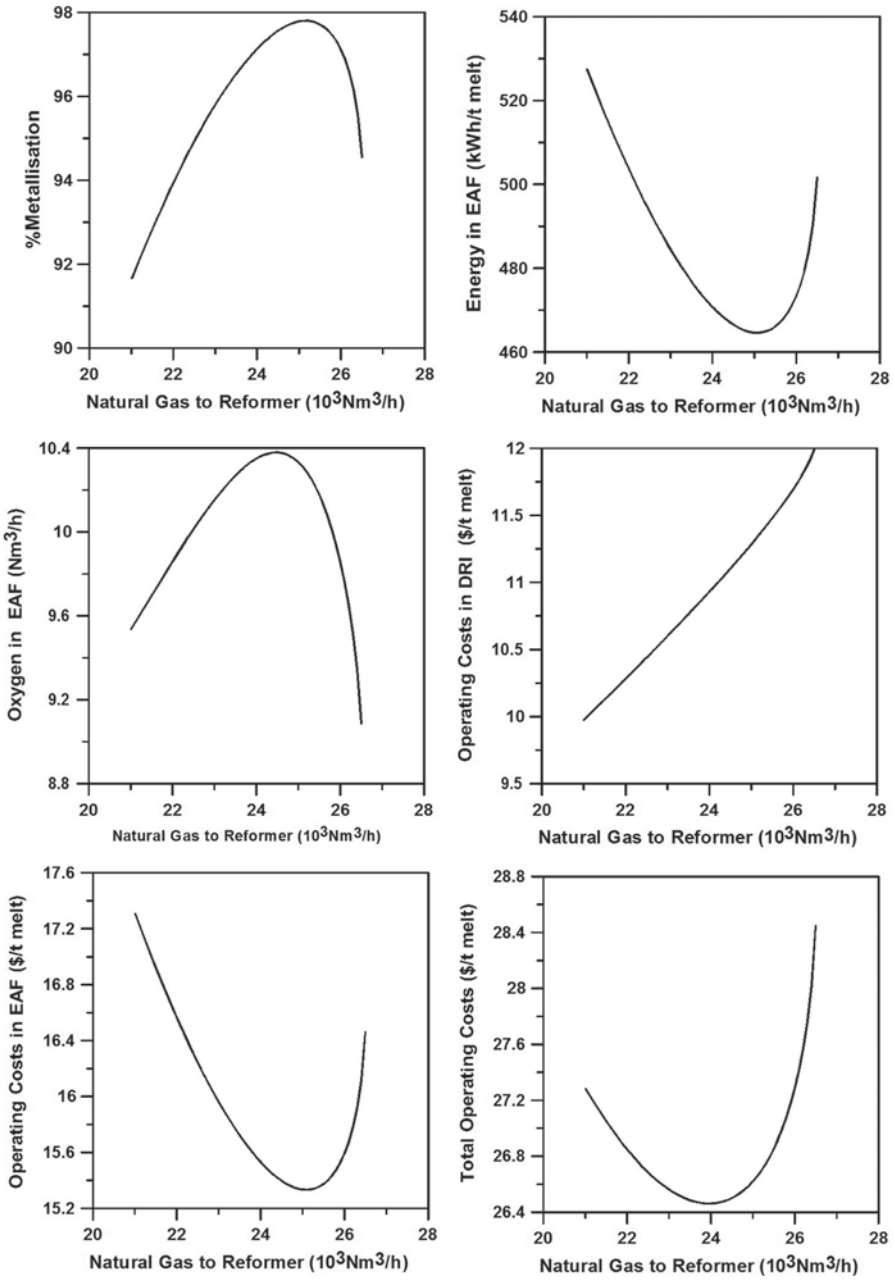

Figure 2. Effect of natural gas flow rate to reformer.

However, as the flow rate of natural gas increases, conditions causing less reforming in the reduction furnace occur due to the limited capacity of the reformer. This leads to lower reductants-to-oxidants ratio. Also, because of the limited capacity of the recuperators, reformer inlet temperature starts to drop at a certain flow rate. Consequently, the bustle gas temperature starts to drop. The combination of lower

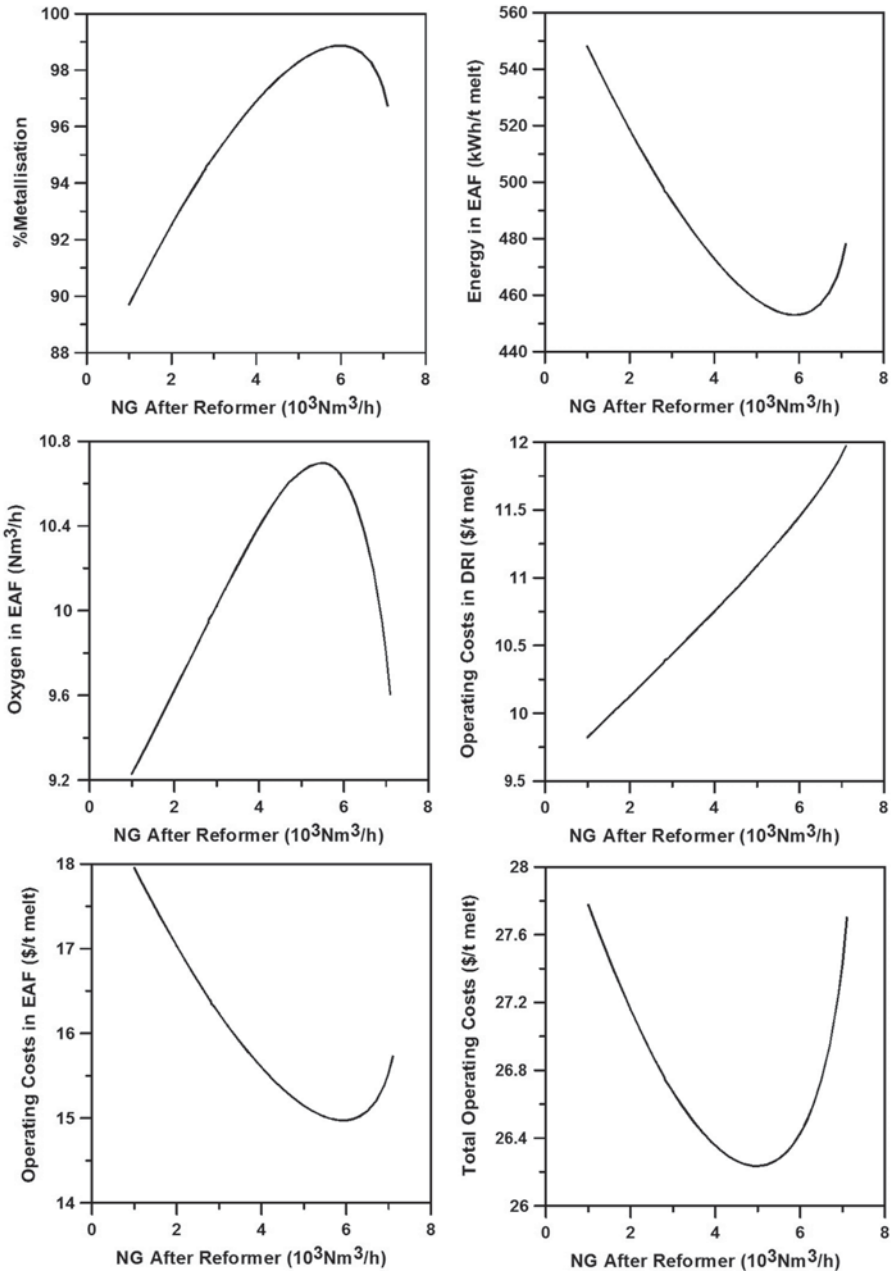

Figure 3. Effect of natural gas flow rate after reformer.

reductants-to-oxidants ratio and lower bustle gas temperature leads to a decrease in metallization and carburization. This leads in turn to an increase in EAF electric energy, less oxygen, less DRI operating costs, and more total operating costs. This explains the maximum in oxygen consumption and the minima in EAF electric energy as well as in operating costs of both the EAF and the integrated plant.

Effect of Injected Oxygen Flow Rate

The effect of injected oxygen is shown in Figure 4. The flow rate was varied in a wide range from 300 to 1700, around the nominal value of 1100 Nm^3/h. As the flow rate of oxygen increases, some reformed hydrogen will burn. This leads to more reduction

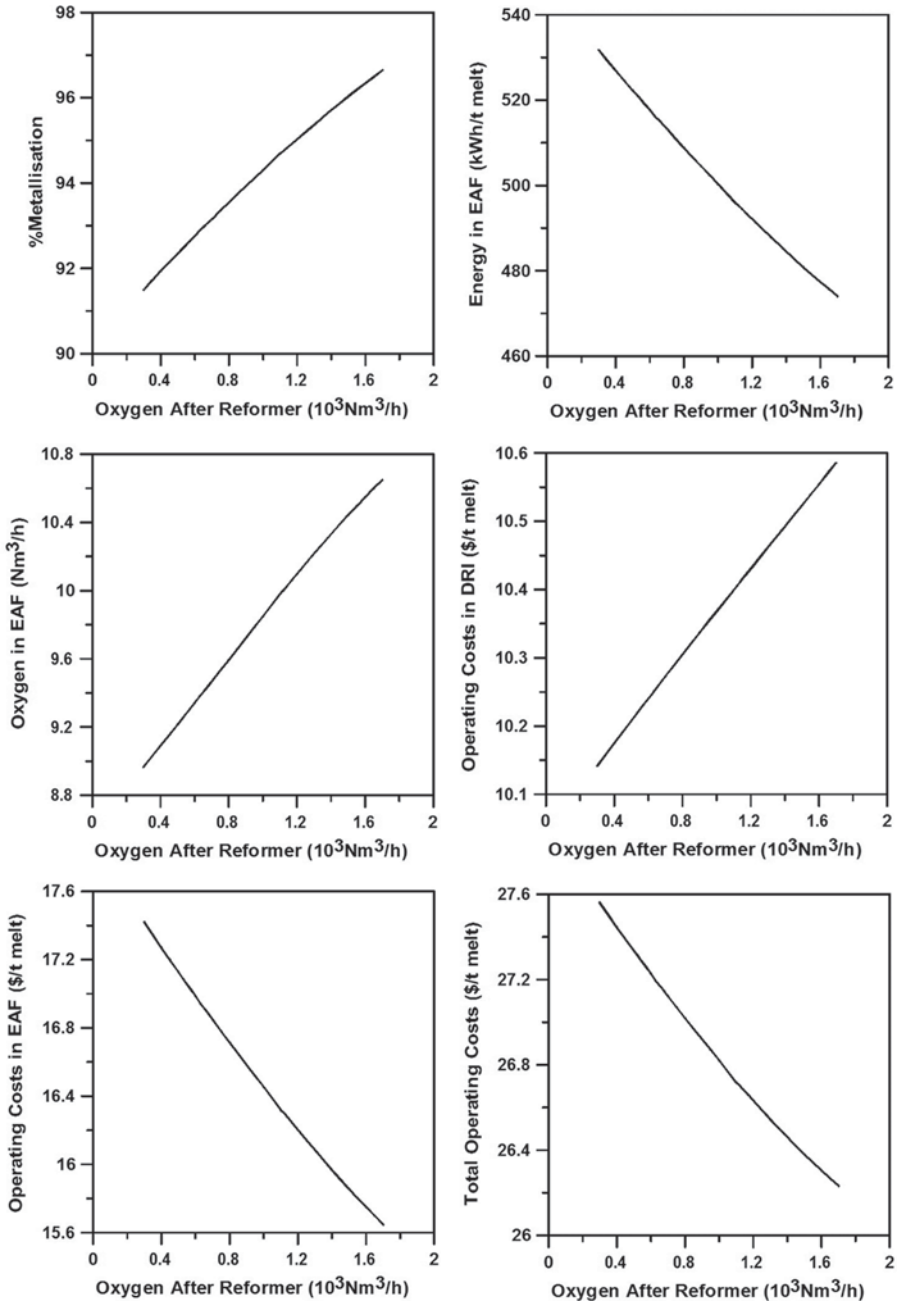

Figure 4. Effect of oxygen injection.

and carburization, which results in an increase in metallization. Increasing the injected oxygen flow rate could also lead to less H_2/CO because of the combustion of hydrogen by oxygen. Lower reformer inlet temperature means less reforming, and less overall flow rates, and hence less compression energy. Because of the additional oxygen cost, the operating cost for the DRI is higher. For the EAF, higher metallization and carbon content lead to a decrease in electrical energy and an increase in oxygen to burn the carbon, which results in less EAF operation cost. The total operating

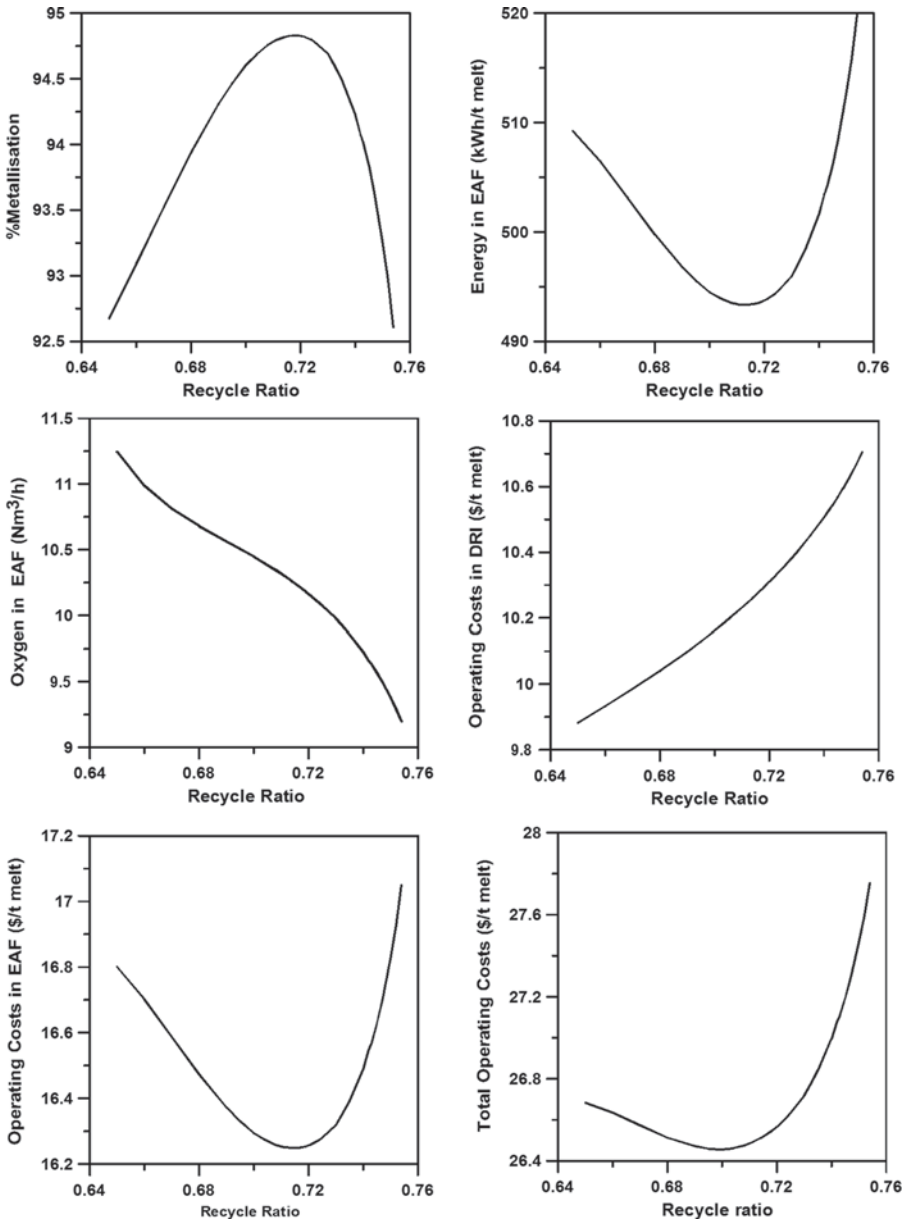

Figure 5. Effect of recycle ratio.

cost is lower because the decrease in EAF operating cost is much more than the increase in DRI operating cost.

Effect of Recycle Ratio

The effect of recycle ratio on the plant performance is shown in Figure 5. The recycle ratio was varied from 0.65 to 0.75 around the nominal value of 0.73. An increase in

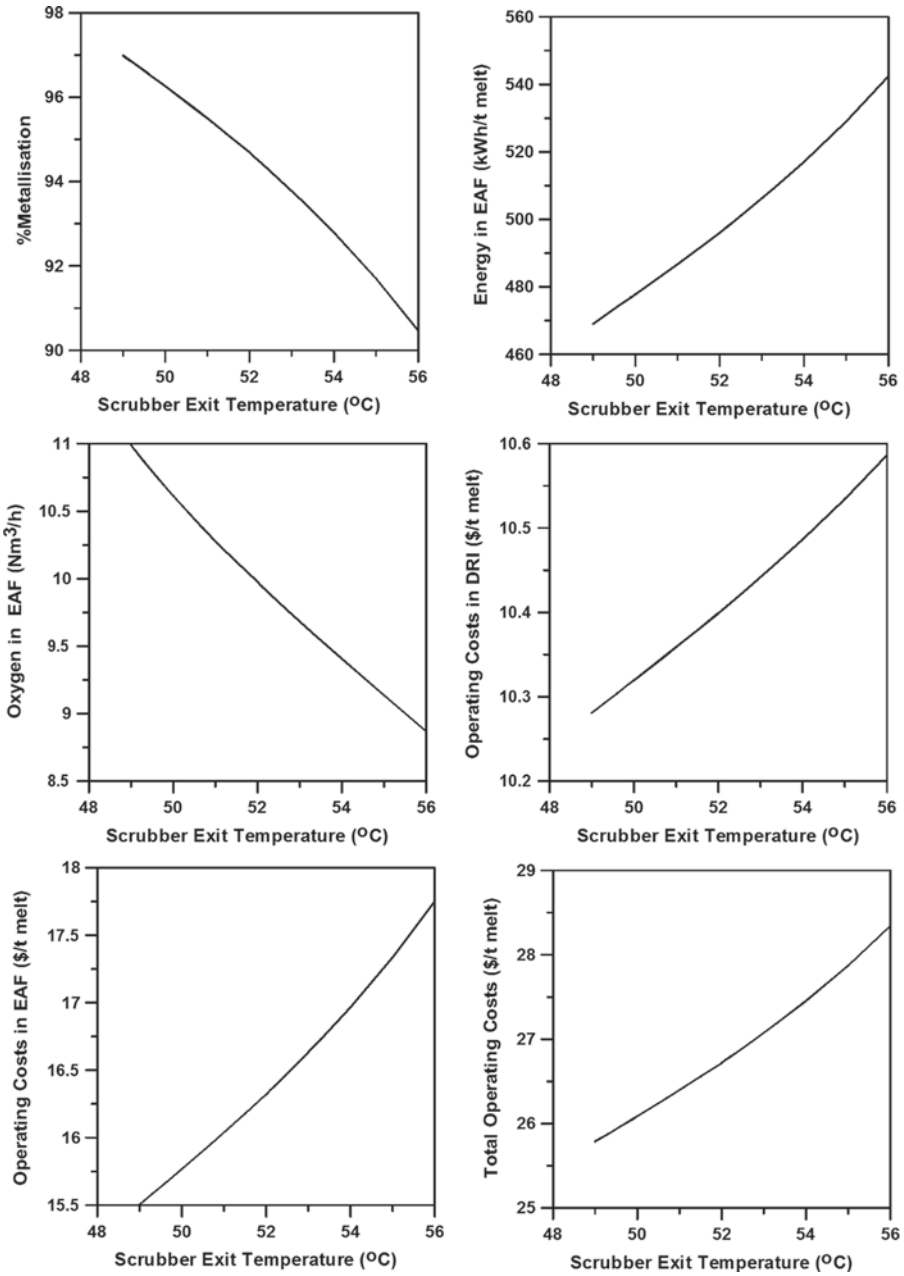

Figure 6. Effect of scrubber exit temperature.

the recycle ratio leads to a lower amount of fuel to the reformer furnace, which means less reforming, less metallization, and more compression energy. However, there will drier reforming than steam reforming and thus lower H_2/CO. This means higher temperature inside the reduction furnace because more reduction takes place by the exothermic CO reduction. Higher reduction temperature in the furnace would

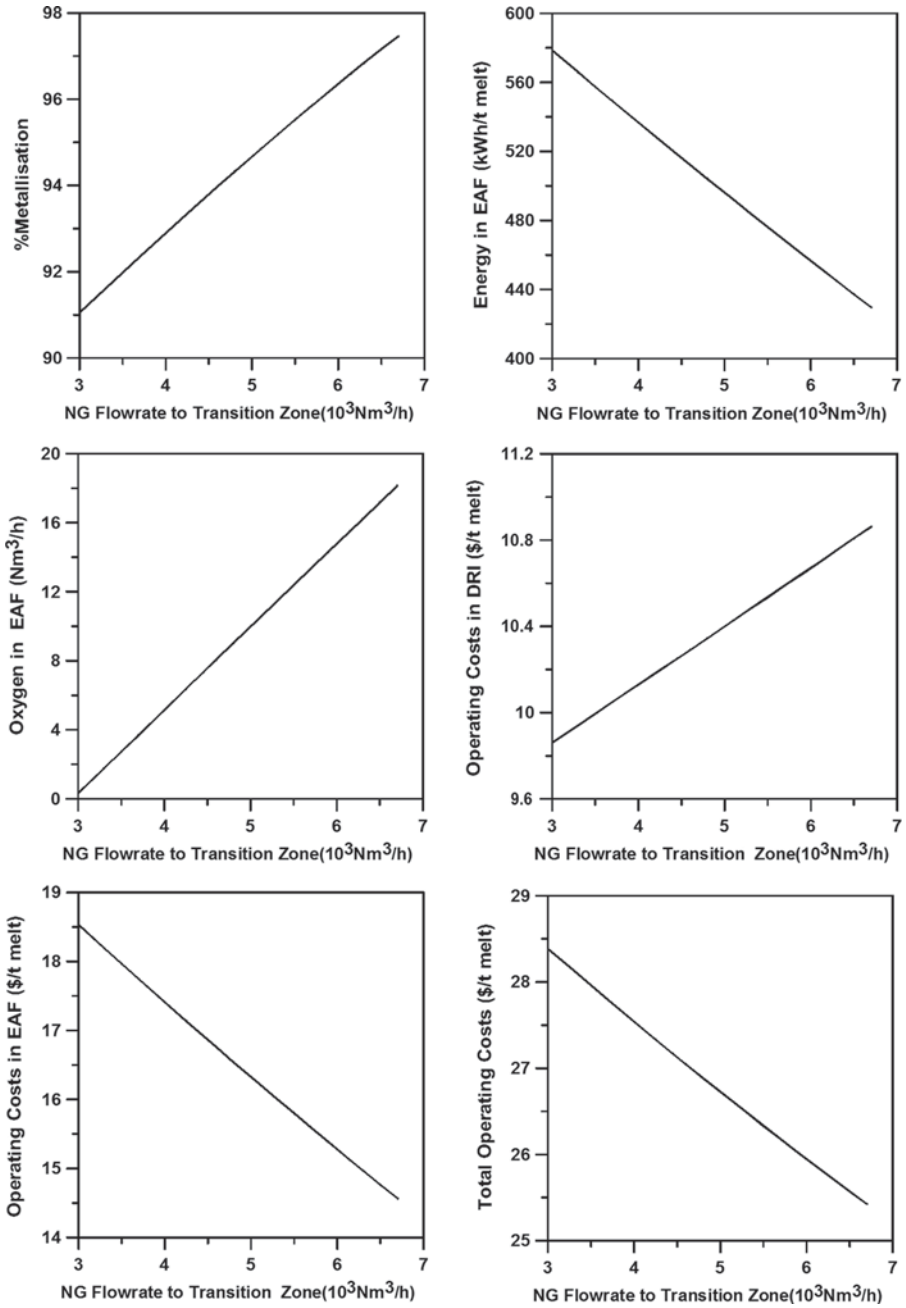

Figure 7. Effect of natural gas flow rate to transition zone.

cause higher metallization, which is in conflict with lower metallization because of lower bustle gas temperature. This is why metallization shows a maximum with an increase in the recycle ratio, and this why electric energy in the EAF shows a minimum. It can be seen that while the operating cost of DRI increases with the recycle ratio that of the EAF shows a minimum (following the minimum in the electric energy). The overall cost, on other hand, shows a minimum at the recycle ratio of 0.70.

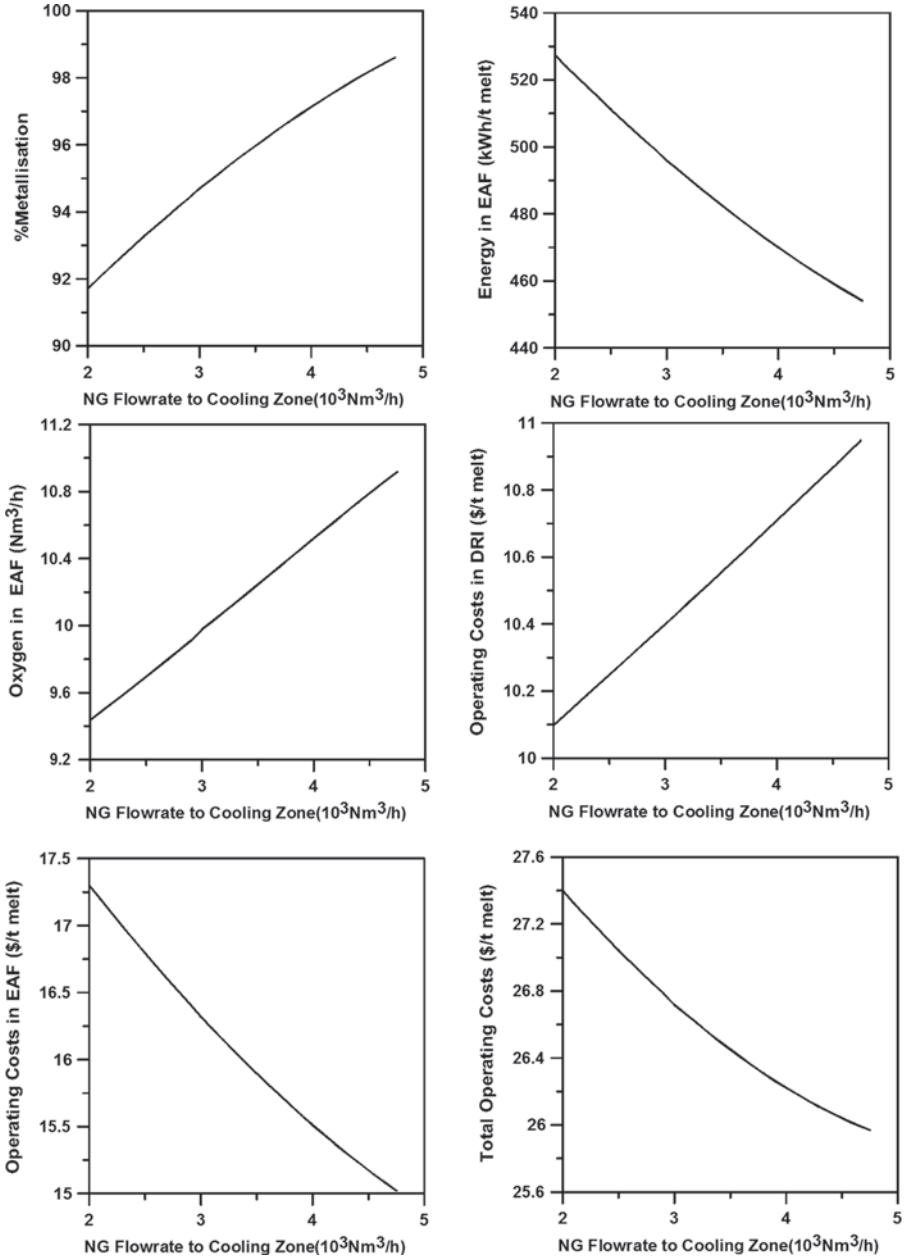

Figure 8. Effect of natural gas flow rate to cooling zone.

Effect of Scrubber Exit Temperature

The effect of scrubber exit temperature is shown in Figure 6. The value of this temperature was varied from 49° to 56°C around the nominal value of 52°C. An increase in the scrubber exit temperature means more water vapor in the process gas, more steam reforming, less bustle gas temperature, and less reduction of iron ore. This leads to less metallization, higher compression energy, higher EAF electric energy,

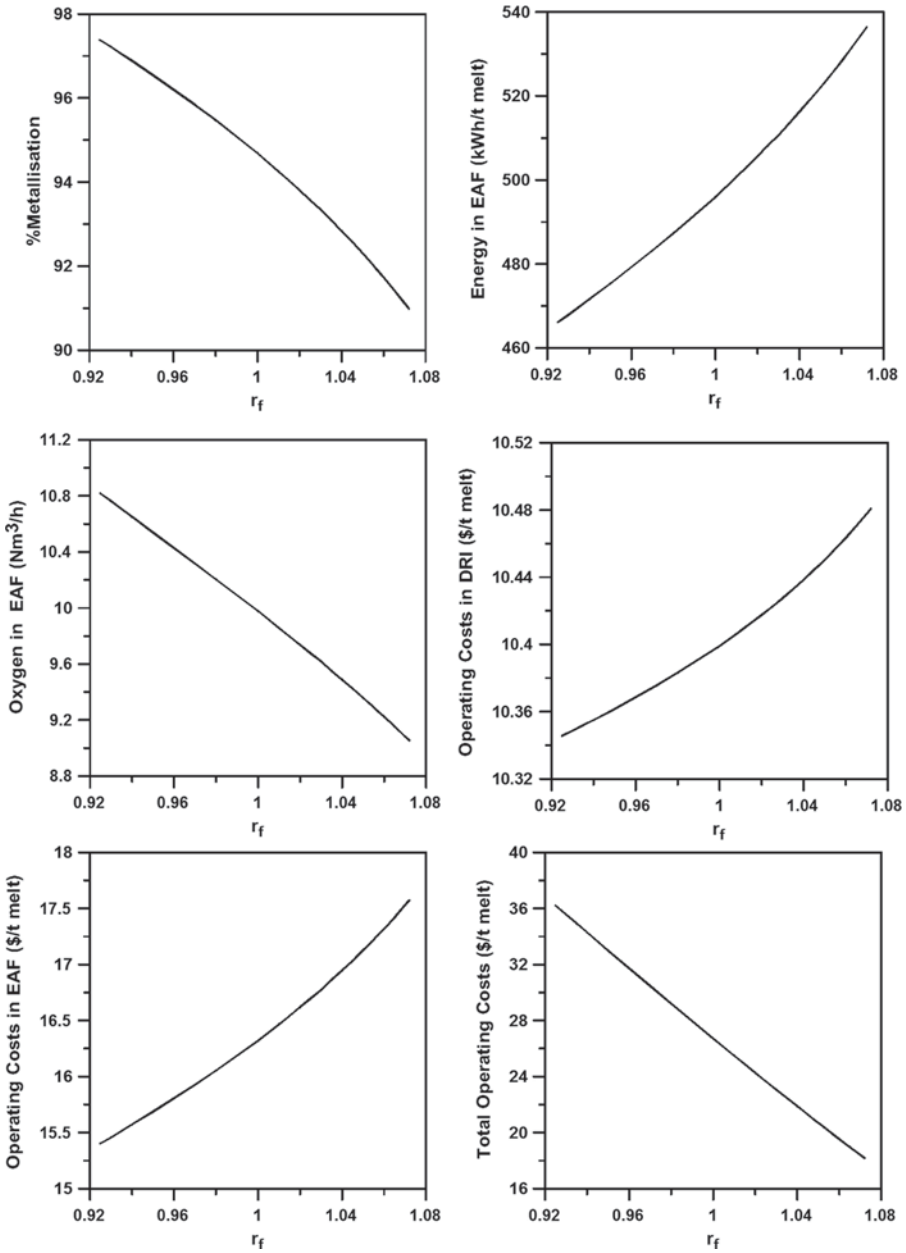

Figure 9. Effect of increase in all input flow rates with the same ratio.

and less required oxygen. The increase in the scrubber exit temperature also leads to higher DRI and EAF and total operating costs.

Effect of Natural Gas Flow Rate to Transition Zone and Cooling Zone

As can be seen in the summary Table VI, these two streams (NG to transition zone and NG to cooling zone) have the same effect on the process. The flow rate to the transition zone was varied from 3000 to 6700 Nm^3/h around the nominal value of 5000 Nm^3/h. The results of the sensitivity analysis are shown in Figure 7. The flow rate to the cooling zone, on the other hand, was varied from 2000 to 4750 Nm^3/h around the nominal value of 3000 Nm^3/h. Figure 8 shows the results of the sensitivity analysis for this stream. Both flow rates, to the transition or the cooling zone, provide hydrogen for the reduction zone due to methane decomposition and thus increase the reductants-to-oxidants ratio. An increase in natural gas flow rate leads to more reforming and more reduction. This means higher metallization, less EAF electric energy, more oxygen, more DRI operating cost, less EAF operating cost, and less total operating cost. Compression energy increases because of the increase of natural gas flow rate and process gas flow rate.

Effect of Increase in All Inlet Flow Rates Including Ore

In this section we present simulation results for the increase in all inlet flows, including the ore flow rate. A parameter (r_f) was introduced in previous sections to represent a ratio multiplying all inlet flows including ore flow rate. The value of (r_f) was varied from 0.93 to 1.07 with unity being the nominal value. The results of the increase in r_f are shown in Figure 9. For a fixed design, increasing the value of r_f means less metallization, less reforming, lower reductants-to-oxidants ratio, and higher compression energy. Although there is an increase in the electric energy of the EAF and an increase in the EAF operating cost, the total cost decreases substantially. This is due to the increase in melt iron production caused by the increase in iron ore flow rate. The value of the production of more iron is much more than the increase in EAF electric energy consumption.

Conclusions

This article attempted to tackle the important and challenging task of the analysis of energy use in an integrated iron/steel plant. The approach followed was to develop models for the integrated plant and then carry out simulation studies. When the individual models were integrated together, the effect of a number of operating parameters on the performance of the plant was clearly identified in appropriate plots and tables. Hence:

- An increase in injected oxygen and natural gas to either the cooling or the transition zone has the same effect. This makes the integrated plant more profitable by decreasing the operating cost of the EAF even if the operating cost of the DRI increases.
- An increase in natural gas flow rate to the reformer, after the reformer, and the recycle ratio has the same effect. Both the costs of EAF and the total operating

costs exhibit a minimum for some values of these operating parameters even if the operating cost of the DRI increases.

- A decrease in scrubber exit temperature lowers the operating costs of the integrated plant as well as the individual operating costs for the DRI and the EAF.
- It can be seen from Figure 9 that it is the change in the parameter r_f that provides the steepest and largest reduction in the total operating cost. The parameter r_f is a ratio multiplying all the inlet flows including ore flow rate. Although its increase causes less metallization, more electric energy consumption in the EAF, and larger operating costs of the EAF, the total cost decreases substantially due to the increase in melt iron production. Therefore, if we have excess EAF capacity, we could increase all input flow rates with the same ratio. Although metallization and carburization decrease, the value of the production of more iron is much more than the increase in EAF electric energy. The question arises, What if the EAF unit is working at its maximum capacity such that we cannot increase the flow rates of all streams? The answer in this case is to increase the injected oxygen flow rate to obtain the maximum permissible bustle gas temperature and to optimize other input streams while avoiding carbon formation in the reformer tubes, a tough constraint indeed. This shows the importance of catalyst research to improve the present reformer catalyst to reduce carbon formation.

Funding

The authors extend their appreciation to the Deanship of Scientific Research at King Saud University for funding this work through the Research Group Project no. RGP-VPP-292.

Nomenclature

C_D	operating costs of DRI per ton of melt iron, \$ t^{-1}
C_{DRI}	operating costs of DRI, \$
C_E	cost of electrical energy, $\$10^{-3}\,kWh^{-1}$
C_{EAF}	operating costs of EAF per ton of melt iron, \$ t^{-1}
C_L	cost of lime, \$ t^{-1}
C_{NG}	cost of natural gas, $\$10^{-3}\,Nm^{-3}$
C_O	cost of oxygen, $\$10^{-3}\,Nm^{-3}$
C_P	selling price of product iron, \$ t^{-1}
C_T	total operating costs of the plant per ton of melt iron, \$ t^{-1}
Ec	energy required for compression, kWh
f_A	natural gas flow rate after reformer, $Nm^3\,h^{-1}$
f_C	natural gas flow rate to cooling zone, $Nm^3\,h^{-1}$
f_O	oxygen flow rate after reformer, $Nm^3\,h^{-1}$
f_R	natural gas flow rate to reformer, $Nm^3\,h^{-1}$
f_T	natural gas flow rate to transition zone, $Nm^3\,h^{-1}$
G_a	weight of gangue, t
G_A	furnace tap weight, t
$G_{A,base}$	base value of G_A, t
G_Z	weight of CaO added, t
O_X	oxygen flow rate, $Nm^3\,h^{-1}$
W_C	weight of carbon in DRI, t

W_{CaO} weight of CaO in excess of G_z to form slag with the excess SiO_2, t
W_{FeO} weight of ferrous oxide, t

References

Adams, W., Alameddine, S., Bowman, B., Lugo, N., Paege, S., and Stafford, P. (2001). Factors influencing the total energy consumption in arc furnaces, paper presented at the 59th Electric Arc Furnace Conference, Phoenix, Arizona.

Ajbar, A., Alhumaizi, K., and Soliman, M. A. (2011). Modelling and parametric studies of direct reduction reactor, *Ironmaking Steelmaking*, **38**, 401–411.

Alhumaizi, A., Ajbar, A., and Soliman, M. A. (2012). Modeling the complex interactions between reformer and reduction furnace in a Midrex-based iron plant, *Can. J. Chem. Eng.*, **90**, 1120–1141.

Bekker, J. G., Craig, I. K., and Pistorius, P. C. (1999). Modeling and simulation of an electric arc furnace process, *ISIJ Int.*, **39**, 23–32.

Çamdali, U., Tunç, M., and Karakas, A. (2003). Second law analysis of thermodynamics in the electric arc furnace at a steel producing company, *Energy Convers. Manage.*, **44**, 961–973.

Czapla, M., Karbowniczek, M., and Michaliszyn, A. (2008). The optimisation of electric energy consumption in the electric ARC furnace, *Arch. Metal. Mater.*, **53**, 599–565.

Dressel, G. L. (1999). Use of DRI in EAFs, Part 4, *Iron Steelmaker*, **26**, 53–55.

Ekmekci, I., Yetisken, Y., and Çamdali, U. (2007). Mass balance modeling for electric arc furnace and ladle furnace system in steelmaking facility in Turkey, *J. Iron Steel Res. Int.*, **14**, 1–6.

Fraser, S. D., Monsberger, M., and Hacker, V. (2006). A thermodynamic analysis of the reformer sponge iron cycle, *J. Power Sources*, **161**, 420–431.

Hocine, L., Yacine, D., Kamel, B., and Samira, K. M. (2009). Improvement of electrical arc furnace operation with an appropriate model, *Energy*, **3**, 1207–1214.

Kirschen, M., Badr, K., and Pfeifer, H. (2011). Influence of direct reduced iron on the energy balance of the electric arc furnace in steel industry, *Energy*, **36**, 6146–6155.

Köhle, S. (2002). Recent improvements in modelling energy consumption of electric arc furnaces, in *7th European Electric Steelmaking Conference*, 1305–1314, AIM, Milan, Italy.

Larsson, M., and Dahl, J. (2003). Reduction of the specific energy use in an integrated steel plant—The effect of an optimisation model, *ISIJ Int.*, **43**, 1664–1673.

Larsson, M., Wang, C., and Dahl, J. (2006). Development of a method for analyzing energy, environmental and economic efficiency for an integrated steel plant, *Appl. Therm. Eng.*, **26**, 1353–1361.

MacRosty, R. D., and Swartz, C. L. E. (2005). Dynamic modeling of an industrial electric arc furnace, *Ind. Eng. Chem. Res.*, **44**, 8067–8083.

MacRosty, R. D. M., and Swartz, C. L. E. (2007). Dynamic optimization of electric arc furnace operation, *AIChE J.*, **53**, 640–653.

Matson, S., and Ramirez, W. F. (1999). Optimal operation of an electric arc furnace, in *57th Electric Furnace Conference Proceedings*, 719–730, ISS Publishers, Warrendale, Penn.

Morales, R. D., Rodríguez-Hernández, H., Garnica-González, P., and Romero-Serrano, J. A. (1997). A mathematical model for the reduction kinetics of iron oxide in electric furnace slags by graphite injection, *ISIJ Int.*, **37**, 1072–1080.

Morales, R. D., Rodríguez-Hernández, H., and Conejo, A. N. (2001). A mathematical simulator for the EAF steelmaking process using direct reduced iron, *ISIJ Int.*, **41**, 426–435.

Morales, R. D., Conejo, A. N., and Rodríguez, H. H. (2002). Process dynamics of electric arc furnace during direct reduced iron melting, *Metal. Mater. Trans. B*, **33B**, 187–199.

Pfeifer, H., Kirschen, M., and Simoes, J. P. (2005). Thermodynamic analysis of EAF, in *8th European Electric Steelmaking Conference*, 211–232, Birmingham, UK.